Mechanism of structure formation in self-propagating thermite reactions: comparison between alumina and silica as additives in the starting mixture

R. Orrù, B. Simoncini, P. F. Virdis and G. Cao
Dipartimento di Ingegneria Chimica e Materiali, Università degli Studi di Cagliari, Cagliari, Italy

Abstract

The mechanism of the self-propagating thermite reaction between aluminum and hematite or the microstructure formation of the reaction products with the same alumina and silica content in the starting mixture are investigated by means of the combustion front quenching technique. It is found that the reactants in powder form are converted into products by passing through different transformation zones with changing microstructure and composition. A relatively detailed structural transformation mechanism for the case of alumina as additive, whose final step is the crystallization of alumina and hercynite from a melt, is postulated. On the other hand, at least at this stage, a result of the same type seems difficult to obtain when considering silica as additive.

Riassunto

È stato affrontato lo studio del meccanismo delle reazioni autopropaganti di tipo termite tra alluminio ed ematite e della formazione della microstruttura dei prodotti, per uguali tenori di allumina o silice nella miscela iniziale, mediante la tecnica dello "spegnimento" del fronte di reazione.
Il passaggio dai reagenti, presenti sotto forma di polveri, ai prodotti finali avviene attraverso diverse zone di trasformazione nelle quali si notano variazioni microstrutturali e compositive.
È stato proposto un meccanismo di formazione della struttura relativamente dettagliato con riferimento al caso dell'allumina quale additivo, che indica come stadio finale quello di cristallizzazione dell'allumina e dell'ercinite dalla massa fusa.
Nel caso in cui si consideri la silice quale additivo, è più difficoltoso proporre, almeno in questa fase, un meccanismo dettagliato.

INTRODUCTION

In the other work submitted together with the present one (cf. Orrù *et al*, 1996c), we have reported the description of the microstructures of the product of the self-propagating thermite reaction between aluminum and ferric oxide at different alumina or silica contents in the starting mixture. As obtained by other researchers (cf. Wang *et al.*, 1993), we also found that this thermite reaction can attain temperatures which are above the melting points of the products that consist of a heavier metallic phase and an oxide phase. This feature, together with the self-sustaining character of the reaction, is exploited in a variety of technological applications such as the synthesis of refractory ceramic and composite materials (cf. Merzhanov, 1990 and reference therein) and the preparation of ceramic linings in metallic pipes (Odawara, 1990; Yin *et al.*, 1993; Chandran *et al.*, 1995; Orrù *et al.*, 1995, 1996a). In fact, the obtained phases can be conveniently separated by gravity when the molten state is reached by taking also advantage of some unique characteristics of self-propagating high-temperature reactions, i.e. low energy consumption, high heating rate (up to 10^6 K/s), short synthesis times (of the order of a few seconds), high product purity and the ability of synthesizing metastable phases (cf. Munir and Anselmi Tamburini, 1989; Merzhanov, 1990; Holt and Dunmead, 1991; Varma and Lebrat, 1992; Merzhanov, 1993). On the other hand, some of these unique aspects, i.e. extremely high temperature gradients and short duration times, make the corresponding process of product formation less controllable as compared to conventional powder technologies. Novel strategies of achieving the desired control of the final products during the corresponding manufacturing processes may be based upon the study of synthesis mechanism. This area of research, which belong to reactions in condensed phase, has recently received considerable attention in the literature (cf. Merzhanov and Rogachev, 1992; Shteinberg and Knyazik, 1992; Rogachev *et al.*, 1993, 1994; Zhirkov and Dovzhenko, 1994; LaSalvia *et al.*, 1995).

As for thermite reactions we started a detailed investigation of the corresponding mechanism of structural transformations during the reduction between aluminum and ferric oxide, since this reacting system has an attractive technological application in the synthesis of wear and corrosion resistant coatings. By using the combustion front quenching technique the study (Orrù *et al.*, 1995, 1996b) was performed for the case when alumina is added to the starting mixture following the recipe of coating synthesis (Chandran *et al.,* 1995). It should be noted that additives have to be present in the starting mixture in order to reduce the violent character of this reaction. It was found that the reactants in powder form are converted into products by passing through different transformation zones. Among final products, alumina and hercynite ($FeAl_2O_4$) seem to be formed as a consequence of a crystallization process from a melt. This study represents a natural extension of previous works and is aimed to describe for the first time experimental data concerning the structural transformations during the reaction between aluminum and ferric oxide in the presence of silica in the starting mixture, since the latter is also used during the coating synthesis mentioned above, because of the formation of lower melting point products with respect to the case of alumina. These results are compared with the corresponding ones obtained also in previous studies using the same weight percentage of alumina under the same experimental conditions.

EXPERIMENTAL SET-UP AND PROCEDURE

The properties of powders used as received to prepare the reacting mixtures are indicated in table 1, reported in Orrù *et al.,* 1996c. A centrifugal mill (Tecnotest, Italy) is used to mix together with acetone as dispersing agent reactants and additives for about six hours. Scanning electron microscopy (SEM) allows us to verify that a good intermixture was achieved. The reacting mixtures prepared under the conditions above were constitued by ferric oxide and aluminum in stoichiometric ratio, according to the reaction

$$2Al + Fe_2O_3 \longrightarrow 2\ Fe + Al_2O_3,$$

and 25 weight percent of additives, i.e. Al_2O_3 or SiO_2. The obtained mixtures, once dried in air in order to totally eliminate acetone, were then pressed inside a cylindrical copper block (105 mm high with a base diameter of 65 mm) with a wedge shaped notch (50 mm high with a base diameter of 20 mm) depicted in fig. 1, using a uniaxial single-acting press (RMU, Italy) at about 10 kN for approximately one minute. The method of quenching adopted in this work to study the dynamics of microstructural transformations makes use of the experimental set-up schematically shown in fig. 1, where beside the copper block described above, a power supply (Belotti, Italy; output 0-100 V), which provide the energy required for reaction ignition, and a computer (Power Macintosh 7200), which drives the power supply in order to produce a well-defined energy pulse, are present.

A total mass of about 14 and 12 grams of the starting mixture was used for the case of alumina and silica, respectively. The corresponding green density of the pellets with conical shape was determined from mass and geometric measurements and was equal to 2.67, and 2.29 g/cm^3, which represent approximately the 51% and 54% of the theoretical value of the mixtures. The combustion reaction, initiated near the wider base of the wedge by means of a tungsten coil (R.D. Mathis Company, USA) connected to the power supply depicted in fig. 1 and programmed to produce an energy pulse by setting 20 volts for about 4 seconds, propagates towards the wedge's apex and is extinguished due to the combination of intense heat removal by the copper block and the shrinkage of the cross section, as schematically shown in fig. 2. Simultaneously, intermediate and final products are quenched and the evolution of the structure during preheating, combustion and post-combustion can be followed by studying product microstructure and composition at different areas relatively to the location of the combustion front.

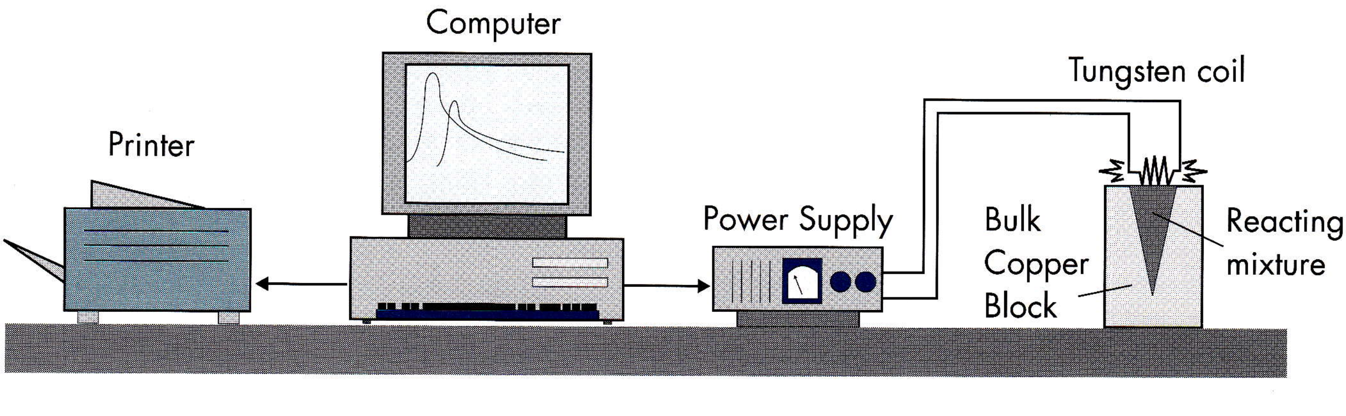

Figure 1: schematic representation of the experimental set-up

Optical metallography (OM), scanning electron microscopy (SEM), wavelength and energy dispersive spectroscopy (WDS and EDS) microanalysis, were employed to analyze samples. Fig. 2 shows schematically the quenched sample area characterized by the techniques above. In order to perform XRD analysis, powder samples were acquired from the same area investigated by the other techniques using several samples quenched under the same experimental conditions and crushed in a mortar. The reproducibility of the experimental runs was verified by repeating each of them at least twice.

RESULTS

Let us consider first the case of alumina as additive in the starting mixture. Some of the results presented here have been obtained in previous works (cf. Orrù *et al.,* 1995, 1996b). The XRD pattern of several samples taken from the area schematically shown in fig. 2, and obtained under the same experimental conditions shows that in addition to aluminum, hematite and alumina, other compounds are detected in crystalline form, i.e. magnetite, wustite and hercynite. In this case, a SEM back-scattered image of the quenched sample from the area of fig. 2 near the combustion front allows us to distinguish the presence of four zones, as shown in fig. 3a - 3b. As moving upwards from the unreacted region (1) the light phase (2) gradually vanishes, thus encountering a single-phase region (3). Region (2) is constitued by aluminum (m) and alumina (n) particles and iron oxides (p), as revealed by WDS microanalysis. These are magnetite and wustite as confirmed by XRD analysis. Aluminum and alumina particles are surrounded by different iron-aluminates (q). These may be considered as the result of the first interaction between the species involved in the aluminothermic reaction. This interaction increases giving rise to amorphous of iron-aluminates (3), where all the alumina of the system is present. In the same region grains of iron and hercynite start to appear. However, these species are present in larger amounts in the heterogeneous region (4). Alumina is present as corundum (x), whose grains grow up to about 10 μm as the distance from the zone (3) increases, being hercynite (y) distributed at the boundary. Iron spots (w) appear to be dispersed in region (4). It is worth noting that final products revealed in the latter region corre-

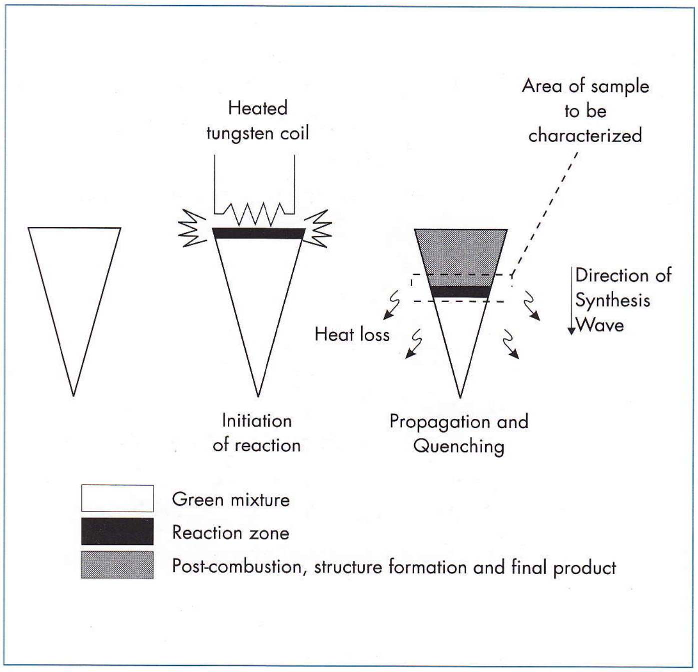

Figure 2: principle of the combustion front quenching technique

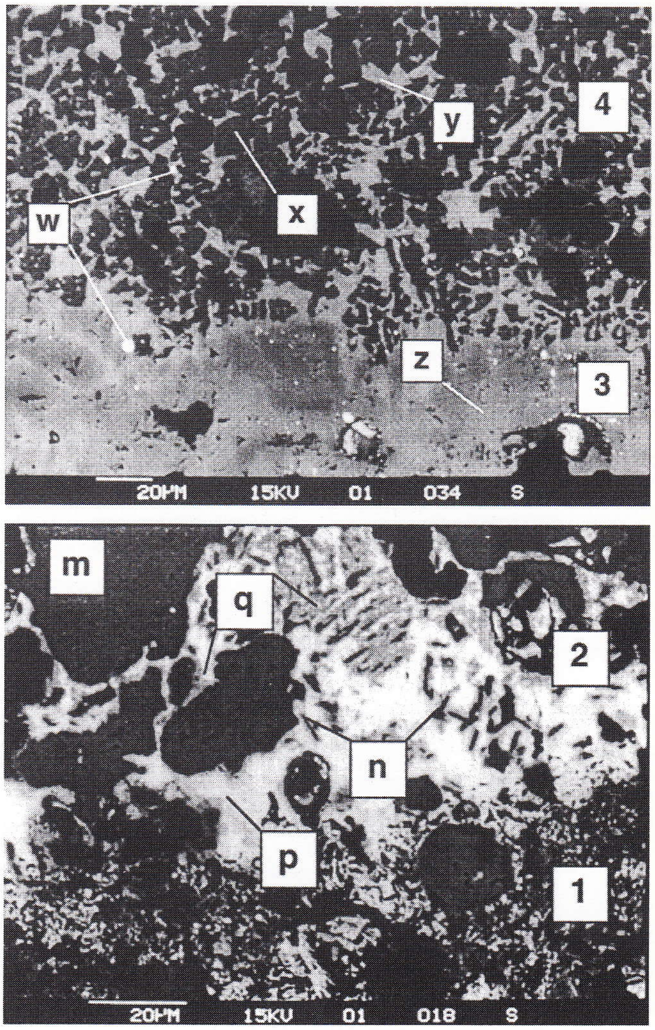

Figure 3: SEM back-scattered views of the lower (a) and upper (b) part where the combustion front is quenched, for the case of alumina as additive: aluminum (m), alumina (n), iron oxides (p), iron-aluminates (q), iron (w), produced alumina (x), hercynite (y) and iron-aluminates as melt (z)

spond to the ones obtained by reacting the same starting mixture without quenching conditions (cf. Orrù *et al.*, 1996c).
Next we consider the case of silica as additive in the starting mixture. It was found that the reaction was stopped not only in the area schematically shown in fig. 2, i.e. moving towards the apex of the wedge, but also close to the copper walls. We examine in the following the area in the neighbourhood of the combustion front, by first performing a XRD analysis, whose pattern is shown in fig. 4. The results indicate that the only species detected in crystalline form, apart from those used to prepare the starting mixture, i.e. aluminum, hematite and silica, were magnetite (Fe_3O_4) and iron. A SEM back-scattered image of this region, which appears to be highly porous, is shown in fig. 5a. The unreacted region (1) is followed by a lighter zone, where the microstructure gradually changes moving upwards from zone (2) to (5).
A more detailed view of regions (1) to (3) of fig. 5a, is shown in fig. 5b. The same figure is also reported in fig. 6 together with the corresponding Fe-Kα, Al-Kα and Si-Kα images.

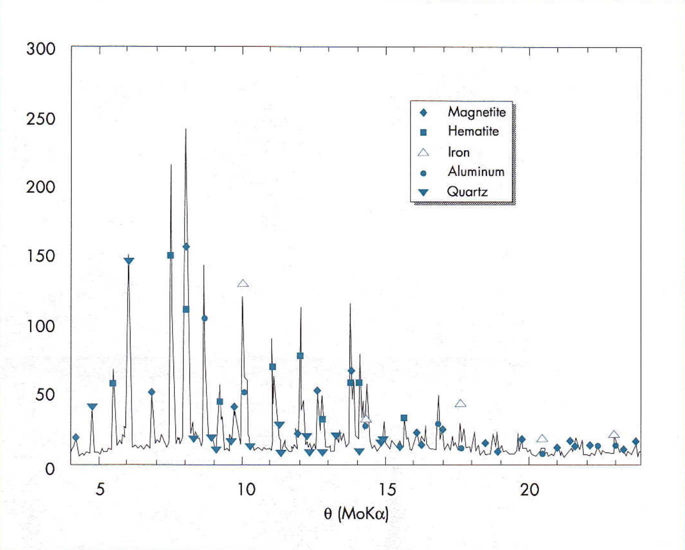

Figure 4: XRD pattern of the powders corresponding to the area schematically shown in fig. 2 where the combustion front is quenched, for the case of silica as additive

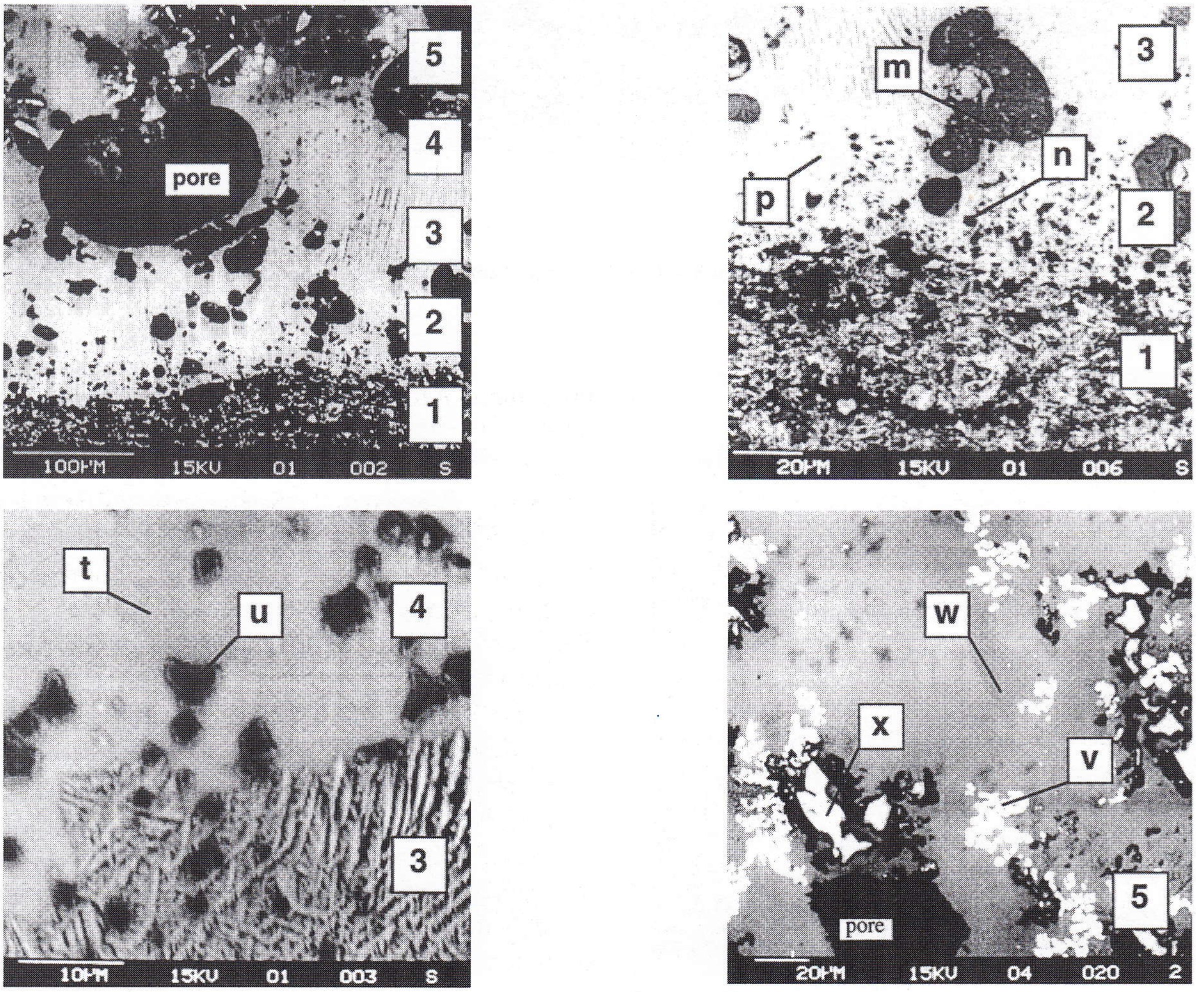

Figure 5: SEM back-scattered micrographs of the area schematically shown in fig. 2: the global quenched region (a), the lower (b), the intermediate (c) and the upper part (d), for the case of silica as additive; aluminum (m), silica (n), iron oxides (p), iron-rich iron silico-aluminates as melt (t), alumina-rich iron silico-aluminates (u), iron (v), iron silico-aluminates as melt (w) and Fe_3Al (x)

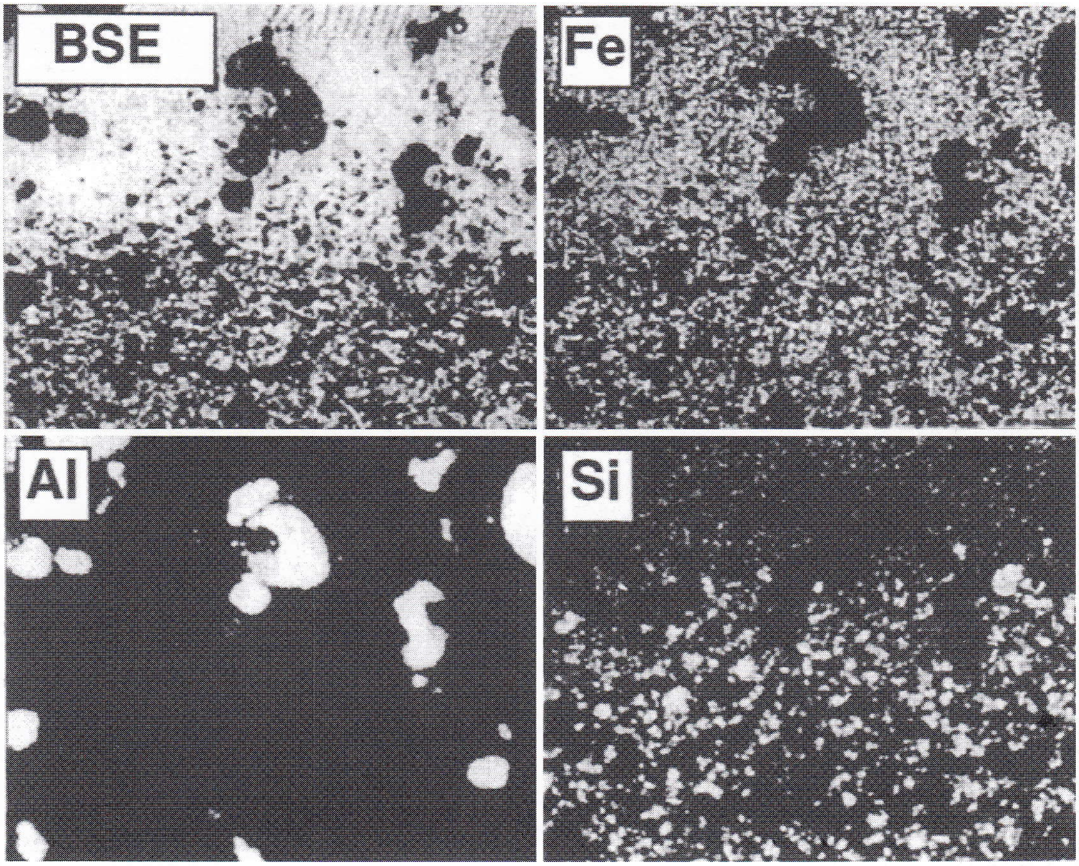

Figure 6: SEM back-scattered, Fe-Kα, Al-Kα and Si-Kα images corresponding to the region reported in fig. 5b

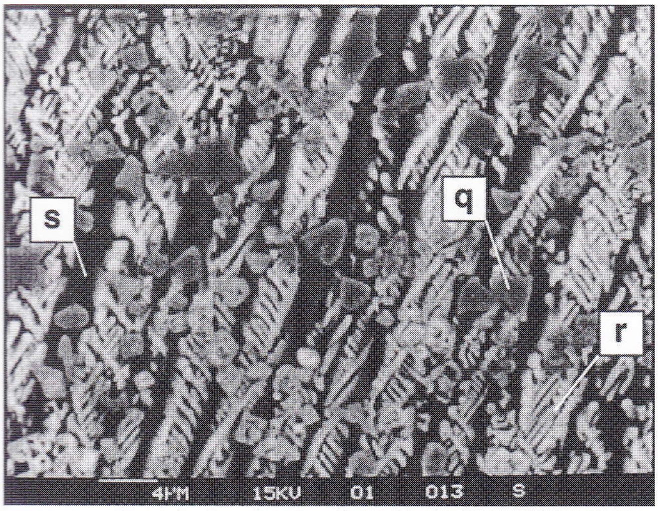

Figure 7: SEM back-scattered detailed view of the region 3 of fig. 5: aluminum-rich iron silico-aluminate phase (q), iron-rich iron silico aluminate phase (r) and iron silico-aluminates (s)

From these, it follows that region (2) of fig. 5b is constitued by aluminum (m) and silica (n) particles dispersed in an iron oxides phase (p).

As clearly observed in the Si-Kα image of fig. 6 it is apparent that silica gradually reacts moving from region (2) to (3) of fig. 5b, thus forming silicates, while aluminum particles are only partially reacted.

The interaction among silicates, aluminum particles and iron oxides, results in a very peculiar structure, corresponding to the upper part of fig. 5b and the lower one of fig. 5c. A detailed view of this region is shown in fig. 7, where three different phases indicated by (q), (r) and (s), may be distinguished. Taking into account the corresponding Fe-Kα, Al-Kα and Si-Kα images reported in fig. 8 and the WDS microanalysis, it is apparent that (q) is an iron silico-aluminate phase, with a high alumina content being the atomic ratio aluminum / iron and silicon / iron equal to 1.4 and 0.12, respectively. On the other hand, phase (r) is an iron-rich iron silico-aluminate, while phase (s) is constitued by iron silico-aluminates with a low alumina content. In fact in phase (r) the atomic ratios aluminum / iron and silicon / iron are equal

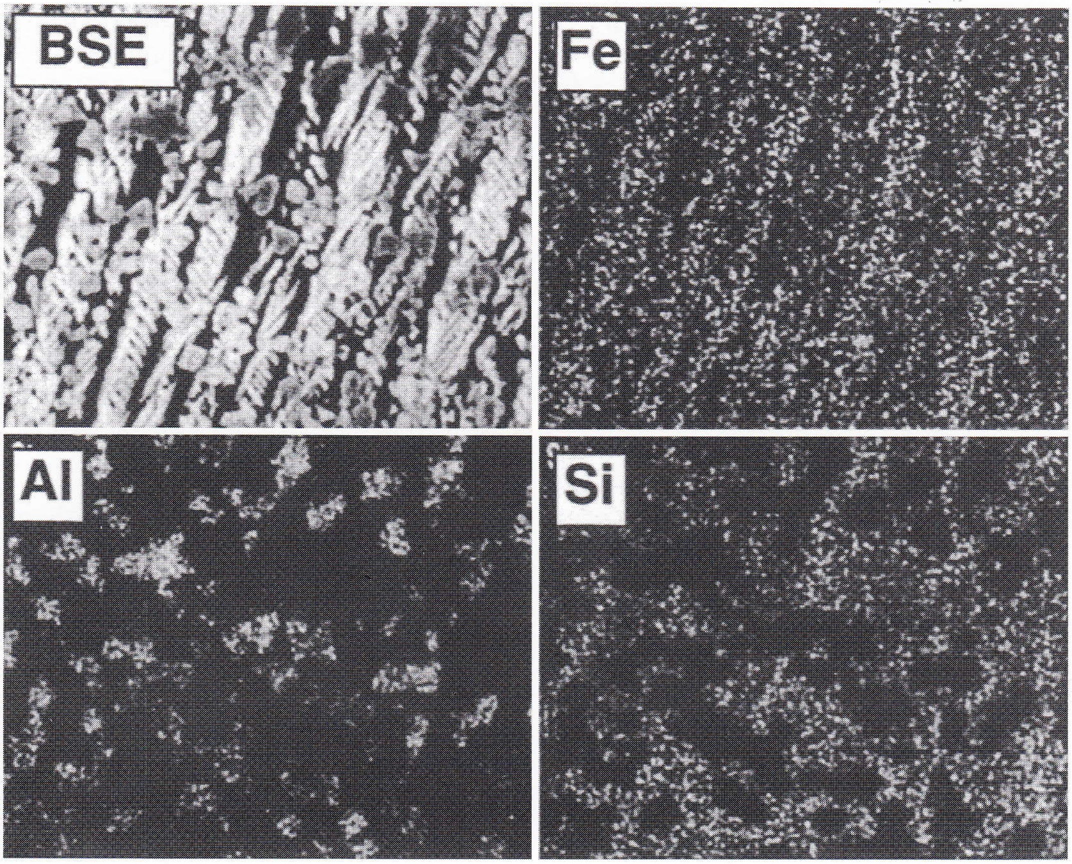

Figure 8: SEM back-scattered, Fe-Kα, Al-Kα and Si-Kα images corresponding to the region reported in fig. 7

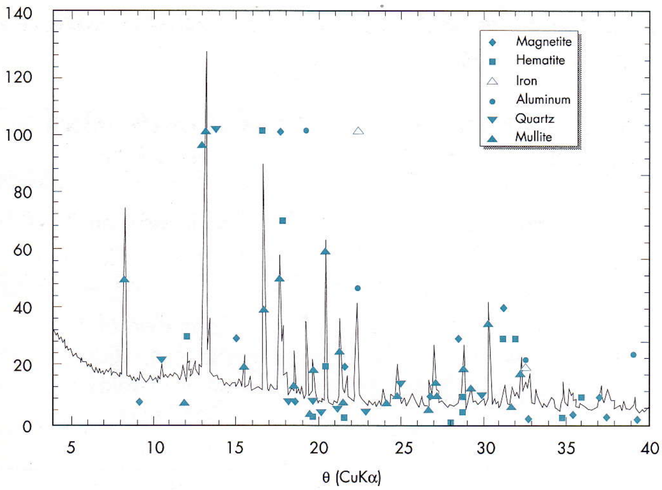

Figure 9: XRD pattern of the powders corresponding to the region quenched near to the wedge copper walls, for the case of silica as additive

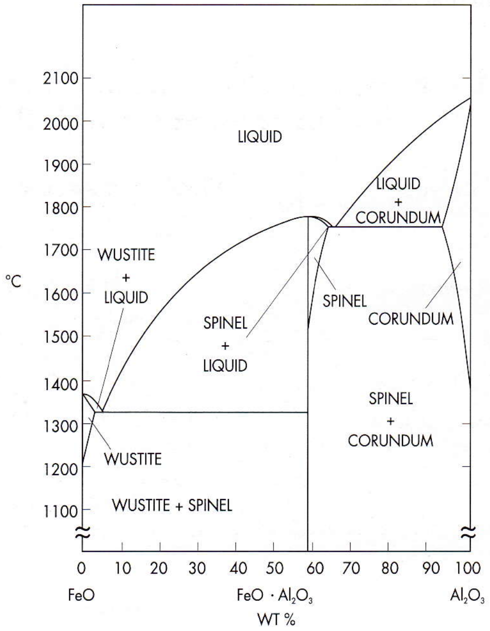

Figure 10: diagram illustrating phase equilibria in the system FeO -$A1_2O_3$ under strongly reducing conditions

temperature with respect to hercynite. Then, the crystallization of the eutectic spinel-corundum takes place. It should be noted that primary alumina undergoes also a continuous grain size increasing, as it may be seen moving upwards in fig. 3b due to more favourable grain grow conditions encountered. The formation of iron may be explained on the basis of equation (3) and (4). The results above may be schematically represented in table 1 where the structure formation zones, which should be passed in order to convert reactants into products, are summarized.

For the case of silica as additive in the starting mixture, a more complex situation with respect to the alumina one is encountered, due to the ability of silica to form amorphous phases with the other oxides. Since these phases are difficult to be characterized relative to the crystalline ones, a mechanism involving such phases is hard to derive. The conversion from reactants into the expected products, i.e. iron and mullite (cf. Orrù *et al.,* 1996c), obtained without quenching conditions, is the result of the formation of various amorphous intermediates, i.e. silico-aluminates of iron, encountered in region (2) and (3) of fig. 5. It may be postulated that these are obtained from the interaction between aluminum and magnetite, which may result from equation (1), as for the case of alumina as additive, together with silica, whose presence does not allow the further reduction of magnetite to wustite. The intermediates mentioned above interact further to form the melt (4) in fig. 5, from which the crystallization of mullite may be postulated. The presence and the mechanism of formation of Fe_3Al and Fe in region (5) are difficult to explain. In the case of silica as additive, it is hard at this stage to propose a detailed mechanism of structural transformations, as presented when considering alumina. In order to achieve this goal, we are currently working towards the direction of reducing the presence of silica in the starting mixture, for which higher quenching rate is required.

ACKNOWLEDGEMENTS

We gratefully acknowledge the financial support from the Regione Autonoma della Sardegna, Italy.

to 0.145 and 0.65, respectively, while in phase (s) the corresponding ratios are 0.59 and 0.88, respectively. Moving from region (3) to (4) in fig. 5c a homogeneous phase of iron silico-aluminates (t) is encountered (aluminum / iron and silicon / iron atomic ratios equal to 0.37 and 0.78, respectively) where small spots (u) of alumina-rich iron silico-aluminates (aluminum / iron and silicon / iron atomic ratios equal to 1.76 and 0.09, respectively) are found dispersed.

Finally, in region (5) of fig. 5d iron (v) is found in the homogeneous phase (w) constitued by iron silico-aluminates, with a much lower iron content with respect to the (t) phase of fig. 5c. Note also that in region (5) of fig. 5d Fe_3Al (x) is also detected.

As mentioned above, the reaction is also stopped near the wedge copper walls. A zone close to such a region was subjected to XRD analysis, whose pattern is shown in fig. 9. It may be clearly seen that we obtain the same results shown in fig. 4 apart from the presence of mullite. Note that this result was expected because mullite ($3A1_2O_3 \cdot 2SiO_2$) and iron are the only products in crystalline form detected by reacting the same starting mixture under "pure" SHS conditions, i.e. without quenching the front (cf. Orrù *et al.,* 1996c).

DISCUSSION

The mechanism of the structural transformations under SHS conditions of the reaction between aluminum and ferric oxide has been studied in the literature only recently (cf. Orrù *et al.,* 1995, 1996b) for the case of alumina as additive. By coupling the information obtained from the various analytical techniques employed together with the study of the interaction of ferric oxide particle on aluminum film using high-temperature diffraction electron microscopy (cf. Korchagin and Podergin, 1979) the following considerations can be made. The formation of magnetite can be explained on the basis of the thermal decomposition of hematite:

$$3\,Fe_2O_3 \longrightarrow 2\,Fe_3O_4 + 1/2\,O_2 \qquad (1)$$

while wustite may result from the subsequent thermal decomposition of magnetite. The formation of hercynite and the simultaneous presence of iron detected moving towards region (z) of fig. 3b may be due to the occurrence of the following reactions:

$$FeO + A1_2O_3 \longrightarrow FeAl_2O_4 \qquad (2)$$

$$1/2Fe_3O_4 + Al \longrightarrow Fe + 1/2FeAl_2O_4 \qquad (3)$$

$$2FeO + Al \longrightarrow 3/2Fe + 1/2FeAl_2O_4 \qquad (4)$$

The formation of iron-aluminates in amorphous form, detected in region (z) of fig. 3b was somehow expected, since the occurrence of phases of this type is typical of SHS reactions. In this case the amorphous phase (z) may be viewed as an intermediate product of the reaction process, which has been "frozen" due to the high quenching rate provided by the copper block in a very short time. Final products detected in region (4) of fig. 3b, i.e. corundum and hercynite, appear then to be formed through a crystallization process from the melt corresponding to the amorphous region (z). From the FeO - Al_2O_3 phase diagram (cf. Fischer, 1956) shown in fig. 10, due to the high alumina content in the melt (atomic ratio aluminum / iron equal to 4.94 as obtained from WDS), alumina crystallizes first because of its higher solidification

TABLE 1 - Representation of transformation zones and their characteristics for the aluminothermic reduction of hematite with 25% of alumina as diluent.

Zones	Chemical species	Nature of structural transformation	Result of chemical interaction
Reactants	Fe_2O_3 Al Al_2O_3	No transformation	No interaction
Intermediate products (1)	Fe_3O_4 FeO Al Al_2O_3 $xFeO \cdot yAl_2O_3$ (y<1)	Chemical reaction	Formation of lower iron oxides iron-aluminates, and iron
Intemediate products (2)	Fe $xFeO \cdot zAl_2O_3$ (y<1<z)	Melting	Completion of reaction
Final products	Al_2O_3 $FeO \cdot Al_2O_3$ Fe	Crystallization and grain growth	No interaction

REFERENCES

1) Chandran, S., Jagarlamudi, S.K. and J.A. Puszynski. Modeling and experimental studies of simultaneous combustion synthesis and densification in the field of centrifugal forces. In P. Vincenzini (Ed.), *Proc. of the 8th CIMTEC-World Ceramics Congress and Forum on New Materials - Ceramics: Charting the Future*, Techna Publ., Faenza, 1995, vol. 3C, pp. 2005-2012.

2) Fischer, W.A. Electrical measurements on oxides and solid cells at temperature of 1200 to 1800 °C. In J.F. Elliot (Ed.), *Proc. of Conf. on the Physical Chemistry of Iron and Steelmaking*, Endicott House, Dedham (Mass.), 1956, pp.79-83.

3) Holt, J.B. and S.D. Dunmead. Self-heating synthesis of materials. *Ann. Rev. Mater. Sci.*, 21 (1991), 305-334.

4) LaSalvia, J.C., Kim, D.K., Lipsett, R.A. and M.A. Meyers. Combustion synthesis in the Ti-C-Ni-Mo system: Part I. Micromechanisms. *Metall. Mat. Trans.*, 26A (1995), 3001-3009.

5) Munir, Z.A. and U. Anselmi Tamburini. Self-propagating exothermic reactions: the synthesis of high-temperature materials by combustion. *Mater. Sci. Rep.*, 3 (1989), 277-365.

6) Merzhanov, A.G. Self-propagating high-temperature synthesis: twenty years of search and findings. In Z.A. Munir and J.B. Holt (Eds.), *Proc. on Int. Symp. on Combustion and Plasma Synthesis of High Temperature Materials.*, VCH Publishers, New York, 1990, pp. 1-53.

7) Merzhanov, A.G. Theory and practice of SHS: worldwide state of the art and newest results. *Int. J. SHS*, 2 (1993) 113-158.

8) Merzhanov, A.G. and A.S. Rogachev. Structural macrokinetics of SHS processes. *Pure and Appl. Chem.*, 64 (1992), 941-953.

9) Odawara, O. Long ceramic-lined pipes produced by a centrifugal-thermit process. *J. Am. Ceram. Soc.*, 73 (1990), 629-633.

10) Orrù, R., Simoncini, B., Virdis, P.F. and G. Cao. Further studies on a centrifugal SHS process for coating preparation and structure formation in thermite reactions. *Int. J. of SHS*, 4 (1995), 137-147.

11) Orrù, R., Simoncini, B., Virdis, P.F. and G. Cao. Computer-aided manufacturing of centrifugal SHS coatings. *Comp. Chem. Eng.*, 20 (1996a), s1185-s1190.

12) Orrù, R., Simoncini, B., Virdis, P.F. and G. Cao. Mechanism of structure formation in self-propagating themite reactions: the case of alumina as diluent. *Chem. Eng. Comm.*, accepted for publication (1996b).

13) Orrù, R., Simoncini, B., Virdis, P.F. and G. Cao. Self-propagating thermite reactions: effect of alumina and silica in the starting mixture on the structure of the final products. *Metall. Sci. Tech.*, accepted for publication (1996c).

14) Rogachev, A.S., Shugaev, V.A., Kachelmyer, C.R. and A. Varma. Mechanism of structure formation during combustion synthesis of materials. *Chem. Eng. Sci.*, 49 (1994), 4949-4958.

15) Rogachev, A.S., Khomenko, I.O., Varma, A., Merzhanov, A.G. and V.I. Ponomarev. Mechanism of self-propagating high-temperature synthesis of nickel aluminides (Part 2): crystal structure formation in a combustion wave. *Int. J. of SHS*, 3 (1994), 239-252.

16) Shteinberg, A.S. and V.A. Knyazik. Macrokinetics of high-temperature heterogeneous reactions: SHS aspects. *Pure and Appl. Chem.*, 64 (1992), 965-976.

17) Varma, A. and J.P. Lebrat. Combustion synthesis of advanced materials. *Chem. Engng. Sci.*, 47, (1992) 2179-2194.

18) Wang, L.L., Munir, Z.A. and Y.M. Maximov. Thermite reactions: their utilization in the synthesis and processing of materials. *J. Mat. Sci.*, 28 (1993), 3693-3708.

19) Yin, S., Liu, M., Yao, C. and Z. Guo. Feldspar additive in ceramic composite pipes made by a centrifugal SHS process. *Int. J. of SHS*, 2 (1993), 69-74.

20) Zhirkov, P.V. and A.Yu. Dovzhenko. Macrokinetics of SHS-product crystallization from the melt. *Int. J. of SHS*, 3 (1994), 167-173.